J. Comput. Appl. Res. Mech. Eng. Vol. 13. No. 1, pp. 75-88, 2023 *DOI: 10.22061/JCARME.2023.9366.2253*

SRTTU

Journal of Computational and Applied Research in Mechanical Engineering

jcarme.sru.ac.ir

JCARME

ISSN: 2228-7922

Research paper

Thermodynamic optimization of an integrated gas turbine cycle, heat exchanger and organic Rankine cycle for co-generation of mechanical power and heating load

Mohammed Ridha Jawad Al-Tameemi*, Samir Gh. Yahya, Saadoon Abdul Hafedh and Itimad D. J. Azzawi

Department of Mechanical Engineering, University of Diyala, Baquba 32001, Iraq

Article info:

Article history:

Received: 19/10/2022

Accepted: 21/04/2023

Revised: 23/04/2023

Online: 25/04/2023

Keywords:

Combined heat and power,

Gas turbine,

Recovery system,

Organic Rankine cycle.

***Corresponding author:**
mohammedridha_eng_@uodiyala.edu.iq

Abstract

A thermodynamic evaluation is conducted on a combined heat and power system integrating a gas turbine (GT), a heat exchanger (HX1), and an organic Rankine cycle (ORC). Traditionally, ORC bottoming GT cycle is limited to mechanical power production. The novelty of this study is to recover wasted heat from the GT cycle in multistage, which is used for the simultaneous production of mechanical power and hot water supply. In the first stage, the HX1 recovers heat from the GT cycle compressed air to heat the water stream. In the second stage, the ORC cycle recovers thermal energy from the GT turbine exhaust stream to produce extra mechanical power with the remaining latent heat used to heat the water. Two models are proposed for comparison using ASPEN Plus software linked with the RAFPROP database. The modelled GT, in this study, is adopted from an actual machine. The steady-state results show that the combined system achieves 51.55% thermal efficiency compared with a standalone GT efficiency, which is only 21%. The thermal efficiency is divided into 24% mechanical power and 27.55% thermal load. The output hot water temperature is 65 ºC. The outcomes of increasing the GT pressure ratio (12-25) are higher combined cycle net power output by up to 16% with a 9.5% reduction in the thermal energy rejected to the environment. Also, the GT efficiency increases from 20% to 22.5%; however, the final water temperature declines from 67 ºC to 60 ºC, which is still appropriate for various heating applications.

1. Introduction

Globally, the demand for energy production is on the rise due to the rapid expansion in population and economy. Coal, oil, and natural gas are the main sources of energy, contributing to more than 80% of the world's total energy supply [1]. Despite the vast investment and growth in renewable energy, oil, and natural gas are expected to remain the main source of energy in the US by 2050 [2]. CO_2 emissions from fossil fuel consumption and the associated global warming are major environmental concerns. In 2019, coal, oil, and natural gas combustion contributed to 44%, 37.7%, and 21.6% of overall CO_2 emissions worldwide [1].

Electricity demand has more than doubled over the past four decades. Approximately 20% of current global energy production is used for electricity, and nearly 68% of this generated electricity is used by the industrial and domestic sectors. Even though electricity production from renewable sources, such as solar, wind, and hydrocarbons is on the rise, fossil fuels remain the main source of fuel for electricity production, accounting for around 61.4% of generated electricity [1]. To reduce fuel consumption and CO_2 emissions, many researchers have focused on improving the performance of power generation systems by utilizing integrated thermodynamics cycles with waste heat recovery technologies, such as CCHP systems [3, 4]. (CCHP) combined cooling, heating, and power system have various advantages, including high efficiency, cost-saving, lower environmental pollution, and wide flexibility in industrial applications due to multigenerational modes [5]. These systems can utilize different prime movers for power generation, such as gas turbines, internal combustion engines, steam turbines, sterling engines, and fuel cells [6]. Most of these prime movers can also be used as heat recovery devices in addition to the heat exchanger, refrigeration, and heat pump systems [3].

Currently, gas turbine combined cycle power plant is one of the most efficient and less pollutant power generation technologies with an operating thermal efficiency of around 60-61% [7, 8]. GT commonly uses natural gas as an energy source to produce mechanical work from the expansion of hot gases in the turbine [9]. The wasted heat in the outlet gases from the GT has the potential to be recovered to produce additional heating, cooling load, and/or power production [10].

Various bottoming cycles have been utilized to recover the wasted heat, such as heat exchanger (HX), ORC as well as various refrigeration cycles like absorption or adsorption cycles. Several studies have employed HX to recover wasted heat from the GT cycle. Aghaei and Saray [11] investigated a GT-driven CCHP system with an auxiliary boiler in a dairy factory using three optimization methods. The results show that the optimized system has higher energy savings and annual total cost savings with lower CO_2 emissions compared to a base design. In addition, it requires a lower compressor pressure ratio of 6 compared to 14.79 in the base design. All three methods demonstrated that air preheater is not necessary and can be removed. Kang *et al.* [12] proposed GT-driven CHP with a ground source heat pump system (GSHP) for the co-generation of electrical power and domestic hot water. HX is used to recover the waste heat from the GT flue gases. The hot water reaches its final temperature through two heating stages. The results support that adopting two heating stages can improve the HP COP from 5.06 to 6.95. In addition, the proposed system can enhance the total energy efficiency by 3.9% with a higher net power output of 669 kW.

Another CHP-GSHP was investigated where the GT wasted heat is recovered by an HX to produce hot water with the remaining heat in the exhaust stream directed to a geothermal well. The proposed system shows an improvement in the first and second law of thermodynamics by 10.7% and 10.4%, respectively, compared to the traditional system [13].

Other researchers have proposed using an ORC as a heat recovery system bottoming a GT cycle to produce additional mechanical power. Balanescu and Homutescu [14] proposed an ORC cycle bottoming 16.5 kW gas turbine power plant to recover the waste heat in the flue gases for additional power production. The results show that the overall system efficiency has increased by approximately 1.1% with better annual fuel and cost savings.

Recently, absorption refrigeration systems (ARS) are widely used as heat recovery systems to produce cooling load. Diyoke *et al.* [15] have proposed two CCHP configurations that integrate GT, ARS, and Biomass power systems (BPS) for cooling, heating, and power production. In the first model, wasted heat from GT and part of BPS is used to heat water for heating applications, while the ARS is powered by the remaining thermal energy rejected from BPS. In model two, the thermal energy in the GT exhaust is used to power the ARS and to produce hot water. The energy efficiency of both proposed models have achieved around 60% and the exergy efficiencies are 17% and 19% for model 1 and 2, respectively. Furthermore, the

proposed system emits 30% less CO_2 than a conventional GT system with a similar capacity. Wang *et al.* [16] proposed a cascade system to recover the wasted heat from the GT exhaust stream. The system consisted of a natural gas driven-GT engine for mechanical power. The wasted heat from the exhaust stream is recovered in two stages. In the first stage, the high-quality thermal energy is recovered to power energy through an ammonia-water turbine, and the exhaust vapor from the first stage powers the LiBr-H_2O absorption system for cooling. In the second stage, hot water is produced from the low-grade thermal energy residual in the GT exhaust stream. The results show that the proposed system can achieve lower fuel consumption by 32% compared with the conventional systems. In addition, the proposed system can manipulate the ratio between power and cooling energy outputs in the range of 1.3-3.3 to suit the customer's flexible requirements.

Another combined GT- absorption HP system has been proposed and investigated for district heating uses. In comparison to the traditional gas boiler, the new system can reduce energy consumption by 6% with an HP COP of 25 [17]. The flue gases of a gas turbine have also been recovered to drive an absorption chiller for heating, cooling, and power production [18].

Other studies suggested using multi-heat recovery systems such as ORC and absorption cooling systems to enhance waste heat recovery from GT cycles. Nondy and Gogoi [5] have proposed two CCHPs that employed a recuperative GT cycle, steam turbine, regenerative ORC, and two absorption cooling systems with a water heater in the first model. While a condensing steam turbine cycle is used instead of the ORC in the second model. In this study, the energy and exergy efficiencies have improved slightly and recorded similar efficiencies and overall energy outputs at the optimum working conditions. While the total cost rate has declined by 9 % and 5.3% with a payback period of around 10 and 13 years for both models, respectively.

A combined micro GT-ORC has been investigated to provide heating, cooling, and electrical energies in a wastewater treatment plant (WWTP). In the winter, the anaerobic digester of the plant utilizes the wasted heat, while in the summer, this energy is used to power an absorption chiller to produce cooling effect. In addition, a by-product hot water is also generated annually. The results show that with higher WWTP capacity, higher payback periods can be achieved but lower energy efficiency [19]. To optimize the real-time performance of a GT combined system, a digital twin approach has been proposed and analyzed. The GT is fuelled by natural gas to produce mechanical energy, while the LiBr-H_2O absorption chiller, hot water, HX and cold energy recovery unit are essential to recover both heat and cold energies of the liquefied CH_4. The results show that the cold energy recovering unit has improved the energy saving rate by 0.72% by recovering additional electrical energy and cooling load. In addition, the digital twin optimization approach has shown an improvement in energy daily rates by 2.23%, 0.35%, and 1.53% during the winter, summer, and transition periods, respectively [20].

Other researchers proposed using solar power to enhance performance and reduce CO_2 emissions from a GT-driven CCHP. Wang *et al.* [21] investigated a solar-assisted CCHP system that integrates a gas Brayton cycle and absorption chiller. The result shows that the combined system has achieved energy and exergy efficiency of around 84% and 25 %, respectively. Another study proposed to use solar power to pre-heat the air entering the combustion chamber, which can reduce the consumption of CH4 and emitted CO_2 gas. The combined system integrates a GT power plant, absorption chiller, Kalina cycle, parabolic solar collectors, and heat recovery heat generator. The findings revealed that the maximum performance can be achieved at GT pressure ratio of 11.6, in addition the PPT in the preheat air, gas turbine inlet temperature (combustion flue gases), and combustion chamber inlet temperature are 11.96 ^oC, 1197 ^oC, and 627 ^oC, respectively. At these working conditions, the combined system has achieved a net power output of 61.73 MW, CO_2 gas emission of 52.87 g/MJ, and exergy efficiency of 44.22% [22].

With the vast improvement in software programs, simulation and analytical studies can

be critical step to identify the ideal design parameters and working conditions of a system prior to experimental studies. For instance, Madani *et al.* [23] conducted a simulation study on the effects of geometry on solid particles in an oil transmission pipeline, which showed that increasing the pipeline diameter decreased the sediment of solid particles. In contrast, increasing the bending radius has increased the sediment of solid particles. Similarly, the design of a centrifugal fan that can be used in many applications, including heating and air conditioning, was simulated using two different geometry [24]. The results show that higher fan efficiency and performance have been achieved by adopting a conical frustum-shape rotor with optimum cone angle, which was validated experimentally. Peiravi and Alinejad [25] have also used simulation analysis to investigate the optimum 3D fiber arrangement in poly matric components (PMC) in terms of thermal conductivity. The thermal conductivity is maximized when the PMC arrangement of triple fiber is perpendicular to heat flux. Another 3D simulation study was conducted on an isothermal cylinder to investigate fluid flow and turbulent natural convection heat transfer under different controlling parameters, such as Nusselt number, Reynold number, and aspect ratio [26]. Similarly, the effect of Reynold number and several shapes of obstacles on the rate of convection heat transfer in an electric board is investigated. The simulation results showed that increasing the Reynold number causes less quantity of energy from the obstacle faces. In addition, decreasing the distance between the obstacles leads to an increase in the rate of convection heat transfer [27].

In this study, a thermodynamic evaluation has been carried out on a combined gas turbine, ORC, and heat exchanger for power and hot water production. The aim is to use the wasted heat recovered from the GT flue gases to heat the water in two heating stages of the ORC and heat exchanger. The additional mechanical power from the ORC is added to the GT power output to enhance the overall net power output of the combined system. For comparison, two models have been proposed with different water inlet and outlet routes to identify the optimum design.

2. Thermodynamic concepts and working principle

The main parts of the proposed combined thermodynamic system are an open gas turbine cycle (GT), an organic Rankine cycle (ORC), and one heat exchanger (HX1), as shown in Fig. 1. The gas turbine cycle is optimized to produce a fixed-rate of a net mechanical power of 5335 kW, while the HX1 and ORC cycle are used to recover the waste heat from the GT flue gases to produce extra mechanical power and thermal load. For comparison purposes, two system models were proposed and investigated. In the first model, the cold water stream (State 11) is first heated by the ORC condenser then the HX1 Fig. 1(a). In the second model, a reverse pathway is proposed where the cold water enters through the HX1 and then ORC condenser Fig. 1(b).

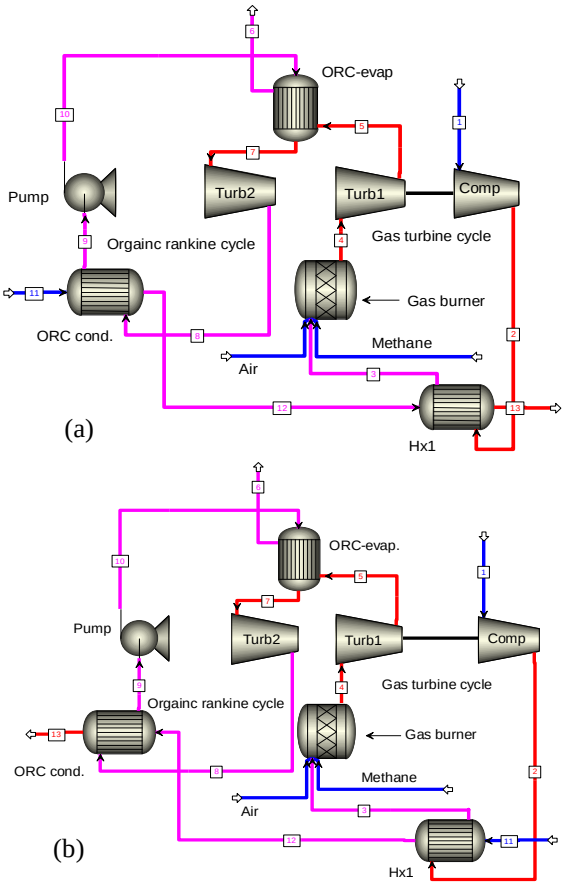

Fig. 1. Schematic diagram of the two proposed combined system with the first heating stage in (a) ORC condenser (b) HX1.

Air enters the GT cycle through Stream 1, then is compressed in the compressor (State1-2) to increase its pressure and temperature, as shown in the TS diagram Fig. 2(a). The high thermal energy available in the compressed air (State 2-3) is transferred by the HX1 to the water stream (State 12-13). After that, the compressed air (Stream 3) enters the gas burner (GB) and mixes with the fuel mixture, where the combustion reaction takes place (State 3-4).

The high-energy fluid exiting the GB (Stream 4) is used to rotate the turbine blade to produce mechanical power through an isentropic expansion process (State 4-5). Part of this mechanical energy is used to power the compressor through direct coupling, while the remaining power represents the GT net power output. However, not all the thermal energy released from burning fossil fuel is converted to mechanical power, and high thermal energy is still available in Stream 5. This thermal energy (State 5-6) is used to thermally power the ORC cycle to produce extra mechanical work while the residual heat in Stream 6 is rejected by the environment to satisfy the second law of thermodynamics.

In the ORC cycle, R245FA is evaporated in the ORC-Evap and converted into a high energy fluid state 10-7, Fig. 2(b). The high kinetic energy of the ORC refrigerant is converted into a mechanical power via the ORC turbine (TURBI2) (state 7-8). The resultant power energy is added to the net power output of the GT cycle to enhance the overall power output of the combined system. The latent heat of the working fluids (state 8-9) is recovered by the ORC condenser to increase the water temperature. Thus, the hot water is produced in two heating stages and its complete route in the combined cycle is streams 11, 12 and 13 for both proposed models. Finally, the working fluid is condensed and pumped to the evaporator (state 9-10) to repeat the cycle.

3. Assumptions and working conditions

The technical specifications and boundary conditions of the GT cycle are adopted from a real cycle model, which is the Centrax gas turbine (CX501-KB7) used for electricity production, as shown in Table 1 [28]. This gas turbine has a net power output of 5335 kW. To achieve the same power capacity of the GT in the combined system, the combined system mass flow rates are iterated until the target GT net power output is achieved. This optimization method is repeated for different GT pressure ratios. ASPEN plus software [29] is used for the modelling procedure, and the REFPROP database [30] is adopted to obtain the thermophysical properties of all working fluids. In addition, an in-house MATLAB code is developed and linked with the same database to obtain the TS diagram for both cycles. Other assumptions and working conditions are listed below:

1. The working fluids for the GT cycle is air, which is consisted of 21% oxygen and 79% nitrogen, while R245fa is selected as the ORC refrigerant [31].
2. Fixed isentropic efficiencies of 80% for the turbines and compressors have been assumed.

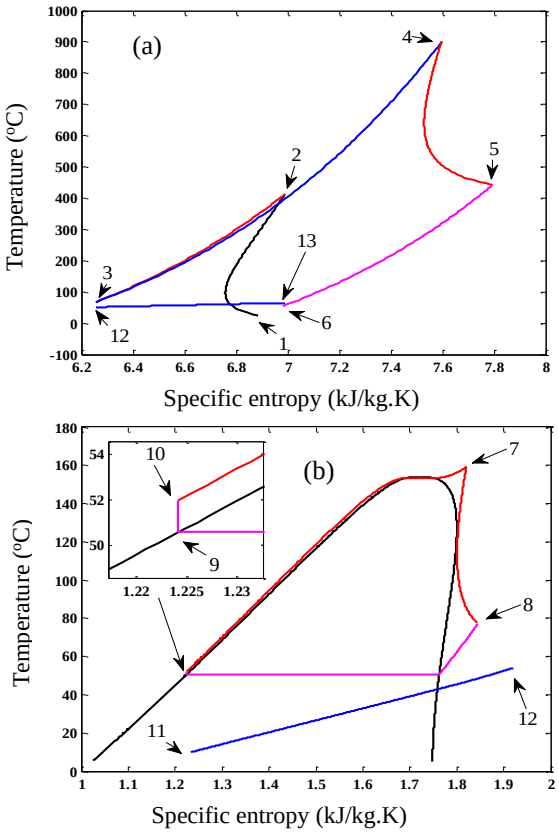

Fig. 2. TS diagram of the (a) GT cycle and (b) ORC.

Table 1. The main technical specification data for gas turbine model (CX501-KB7) [28].

Power output, kw	Pressure ratio, %	Mass flow, kg/s	Exhaust temperature, °C
5335	13.9	21.13	495

3. Mechanical and pressure losses are neglected through all heat transfer processes and mechanical coupling. In addition, no heat loss is assumed except for the heat lost from the GB during the combustion process.
4. The high-pressure side of the ORC cycle is set to a value close to the R245fa critical pressure to achieve the highest cycle performance [32], while the low-pressure side is dependent on the inlet water temperature.
5. A five-degree superheat is assumed at the ORC turbine inlet to secure that no two-phase flow occurs across the expansion process [33].
6. A pinch point approach of 3 °C is assumed in HX1 and ORC condenser [34].
7. The water is assumed to enter the combined system with a temperature of 10 °C and a mass flow rate of 28 kg/s.

4. Theoretical model

Energy balance equations for each cycle components and for the combined system are adopted from open literature [3, 35]. The GT compressor work is calculated as follow:

$$W_{GT\_comp} = \dot{m}_{comp} \times (h_2 - h_1) \quad (1)$$

Thermal capacity of heat exchanger one (HX1) is equal to thermal load transferred to the water:

$$Q_{HX1} = \dot{m}_{comp} \times (h_3 - h_2) = \dot{m}_w \times C_{Pw}\left(T_{w,state\ 13} - T_{w,state\ 12}\right) \quad (2)$$

The thermal capacity acquired from the complete combustion of methane in the burner is evaluated from the following equation:

$$Q_{burner} = (\dot{m}_{comp} + \dot{m}_{fuel\ mix}) \times (h_4 - h_3) \quad (3)$$

GT turbine work is calculated as follow:

$$W_{GT\_turbine} = (\dot{m}_{comp} + \dot{m}_{CH4} + \dot{m}_{Air}) \times (h_5 - h_4) \quad (4)$$

Thermal capacity rejected from GT exhaust stream (5) is used to evaporate the ORC refrigerant in ORC-EVP, as shown in Eq. (5).

$$Q_{ORC-EVAP} = \dot{m}_{total} \times (h_6 - h_5) = \dot{m}_{ORC} \times (h_8 - h_7) \quad (5)$$

The net power output from the GT cycle is the net between the turbine and compressor works, and the thermal efficiency is the ratio between the GT net power output and gas burner thermal capacity:

$$GT_{effe} = \frac{W_{GT-NET}}{Q_{burner}} = \frac{W_{GT\_turbine} - W_{GT\_comp}}{Qburner} \quad (6)$$

ORC condenser thermal capacity equals to the enthalpy difference across the condenser multiplied by the ORC mass flow which is equal to thermal energy transferred to the water:

$$Q_{ORC-cond.} = \dot{m}_{ORC} \times (h_9 - h_8) = \dot{m}_w \times C_{Pw}\left(T_{w,state\ 12} - T_{w,state\ 11}\right) \quad (7)$$

The net power output from the ORC is equal to the net of turbine and pump works, as shown in the below equation.

$$W_{ORC-NET} = \dot{m}_{ORC} \times (h_8 - h_7) - \dot{m}_{ORC} \times (h_{10} - h_9) \quad (8)$$

Total thermal energy gained from the combined cycle:

$$Q_{total} = Q_{HX1} + Q_{ORC-cond.} \quad (9)$$

Total mechanical power produced by the combined cycle:

$$W_{total} = W_{GT-NET} + W_{ORC-NET} \quad (10)$$

Total heat released in the combustion process equals to fuel mass flow multiplied by methane heating value (55.5 kJ/kg):

$$Q_g = \dot{m}_{fuel\ mix} \times Heating\ value_{CH4} \quad (11)$$

The total heat lost in the combustion process and rejected to the environment equals to the mass flow rate multiplied by enthalpy difference between Streams 3-4 and 5-6, respectively. The

combined cycle heat and power energy to total heat released efficiency equal to:

$$CHP_{effe} = \frac{W_{total}+Q_{total}}{Q_g} \quad (12)$$

5. Results and discussion

5.1. Steady-state analysis

In this section, the steady-state results for both proposed models are presented and compared at constant GT pressure ratio and GB exhaust temperature of 14 and 900 °C, respectively. Table 2 shows the main thermophysical properties of the working fluids (air, R245fa, and water) at each state across the combined system. The results show that in States 1, 2, 4, 5, 7, 11, and 13, the properties of the working fluids are similar due to the adopted assumptions. However, the temperature of air at the HX1 exit (State 3) is set to 68 °C in model (A), which secure a PPT of 3 °C with the heated water. While in model (B), this temperature is set to 27.6 °C, which represents the first heating stage. In addition, the differences in exhausted air temperature between both models in State 6 is based on securing a 3 °C PPT with the R245fa temperature in State 10. The condensation pressure and temperature of ORC at State 8 in both models are set according to the designed water temperature in Stream 12. Furthermore, in model (A), the ORC condenser is responsible for the first heating stage. Reducing the condenser pressure and hence temperature at State 9 will increase the ORC efficiency according to Carnot law but will reduce the heated water temperature and vice versa. So, a trade-off condensation temperature value is selected to secure the balance between the two designed parameters. While in model (B), the ORC condenser is in the last heating stage; therefore, the condensation pressure in State 9 is set to a value higher than that in model (A), as given in Table 2.

Table 3 represents the thermal loads and power capacities of the main components of the combined system, the efficiencies of the individual cycles, and the combined system for both models. It shows that for model (A), the total energy recovered (heat and power), which is the sum of the net power output of GT and ORC, and the thermal capacities of HX1 and ORC condenser, equals to 13,108.563 kW, while the total rejected thermal energy is 12,315.753 kW. For model (B), both these values are slightly higher than in model (A), the total energy recovered is 13,167.441 kW and the total energy rejected is 12,371.076 kW. This is contributing to the fact that the total heat released from GB in model (B) is slightly higher than that in model (A). The standalone GT thermal efficiency is only 21%, and by adding the ORC net power output, this value increases to 24%. The percentage between the total energy gained over the total heat released for both models is 51.55 %, indicating a significant improvement in the overall combined system thermal efficiency. The results support that both models can produce similar overall combined system efficiency with a final hot water temperature of 65 °C.

Table 2. Integrated cycle's properties at different states across the combined system.

State	Model (A)		Model (B)	
	T (°C)	P (bar)	T (°C)	P (bar)
State 1	25	1	25	1
State 2	416	14	416	14
State 3	68	14	27.6	14
State 4	900	14	900	14
State 5	441	1	441	1
State 6	55.6	1	68	1
State 7	159	36	159	36
State 8	78.9	3.5	86.7	5
State 9	50.8	3.5	63	5
State 10	52.6	36	65	36
State 11	10	1	10	1
State 12	51.3	1	24.6	1
State 13	65	1	65	1

Table 3. The combined cycle design parameters.

Parameters	Model (A)	Model (B)
Total heat released in GB, kW	25424.32	25538.52
GT turbine work, kW	7264.66	7188.386
GT compressor work, kW	1929.66	1853.386
ORC network output, kW	788.096	687.86
HX1 thermal capacity, kW	1734.817	1857.095
ORC condenser thermal capacity, kW	5250.65	5287.486
Total heat rejected in Stream 6, kW	432.254	602.292
Total heat lost in combustion process, kW	11883.499	11768.784
GT cycle, %	20.9	
Combined cycle, %	51.55	

5.2. Optimization analysis through varying GT pressure ratio

In this section, the effects of varying GT compression ratios on the combined cycle design factors and cycle efficiency are presented and discussed. The modeling procedure is carried out on model (A) by increasing the GT compression ratio from 12-25 bar while maintaining the GT network output constant at 5335 kW. Fig. 3 shows the effect of increasing the GT pressure ratio on the GT compressor and turbine works.

The results show that by increasing the GT pressure ratio, more power is produced by the turbine and compressor. This is because the rise in pressure ratio causes an increase in the enthalpy at the compressor outlet and turbine inlet, resulting in a rise in both devices' power. However, the rise in the compressor consumed work is lower than the rise in turbine produced power as the turbine mass flow rate is higher, as shown in Eq. (4).

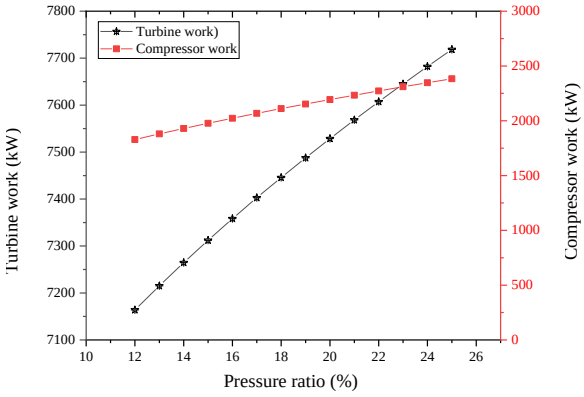

Fig. 3. GT PR correlation to turbine and compressor works.

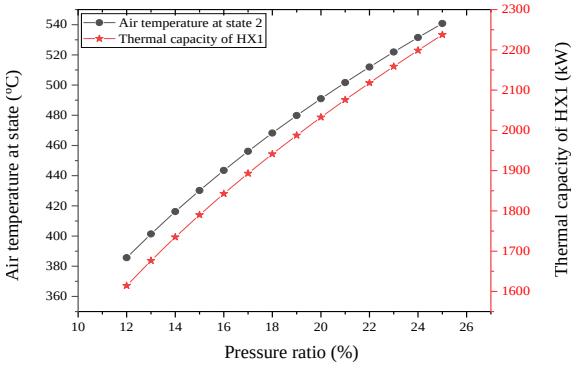

Fig. 4. GT PR correlation to HX1 air temp. and thermal capacity.

For each selected pressure ratio value, the difference between the turbine and compressor works is equal to 5335 kW, which shows that the modeling procedure has satisfied the design requirements.

Fig. 4 shows the effect of varying GT PR on working fluid temperature at State 2 and HX1 thermal capacity. As the pressure ratio increases, both parameters rise dramatically. This is due to the increment in the compressor work, as shown in Fig. 3. Higher compressor work leads to higher air enthalpy at the HX1 outlet, which results in higher temperature and thermal load. The quantity and quality of the HX1 thermal capacity have the potential to be recovered and used in heating applications.

Fig. 5 shows that as the GT-PR increases, the compressor and turbine mass flow rates decline. With increasing the pressure ratio, both works and enthalpy differences increase; however, the rise in enthalpy difference is greater than the rise in each device work, as shown in Eqs. (1 and 4). Fig. 6 shows the total heat added to the water and the total mechanical power gained from the combined cycle.

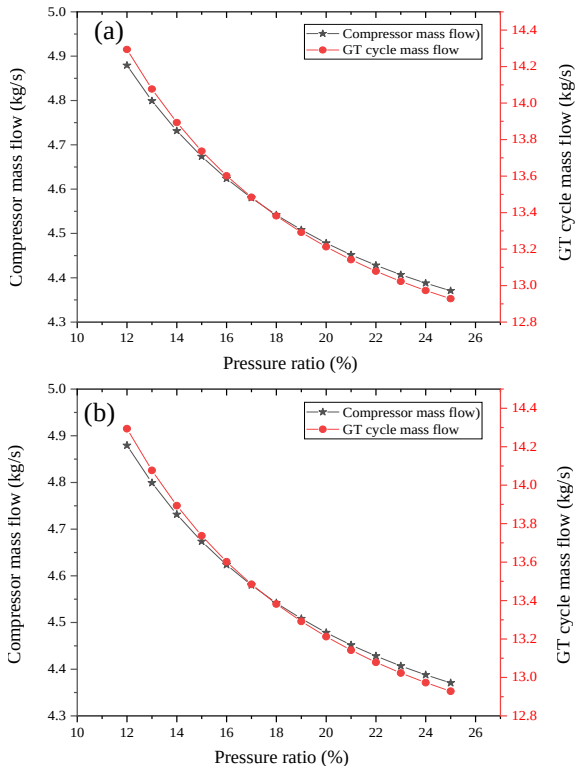

Fig. 5. GT PR relation to (a) turbine and (b) compressor mass flow.

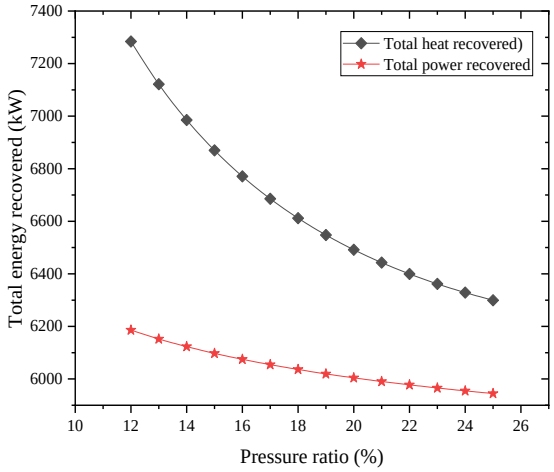

Fig. 6. GT PR to total heat and power recovered.

It shows that the total net power output is greater than the designed GT network output (5335 kW) by around 11.5-16%, which represents the ORC net-work output.

In addition, the integrated cycle has recovered more thermal energy than mechanical power. With a higher GT-pressure ratio, the thermal energy added to the water declines by 13%, which is lower than the decline in the network output of the combined cycle (4%).

Fig. 7 shows the total energy gained and lost across the combined cycle. The energy gained is the sum of the total mechanical powers and total thermal energies added to the water by the combined cycle. While the energy lost is the thermal energy lost in the combustion process and the residual thermal energy rejected from the exhaust. The results show that the total energy gained is higher than the energy lost; however, both energy declines in a similar trend, as the pressure ratio increases.

Fig. 8 shows the behavior of the ORC evaporator (ORC-EVAP) thermal capacity and the rejected thermal capacity to the environment via Stream 6. As the GT pressure ratio increases, both thermal capacities decline due to the decrease in the mass flow rate of the combined cycle (see Fig. 5). Also, increasing the pressure ratio reduces the thermal energy rejected to the environment by the combined cycle by around 9.5%.

The relation between the total thermal energy released from CH_4 burring in the combustion chamber and the CH_4 mass flow to GT-pressure ratio is shown in Fig. 9. The total heat released represents the integration of energy gained and energy lost (Fig. 7).

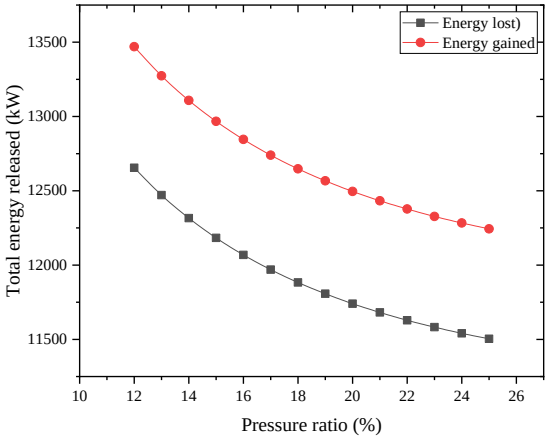

Fig. 7. GT PR relation to total energy lost and gained,

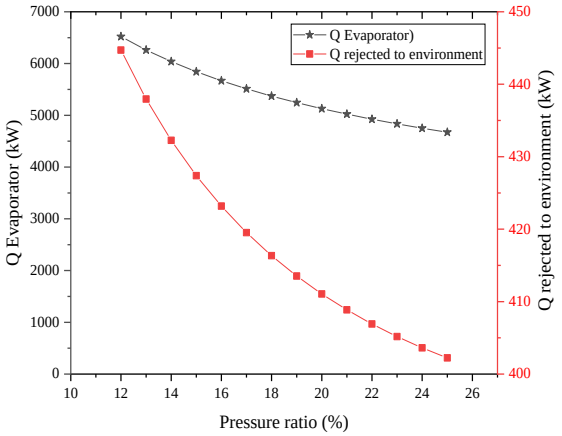

Fig. 8. GT PR to ORC evap. thermal capacity and heat rejected to environment.

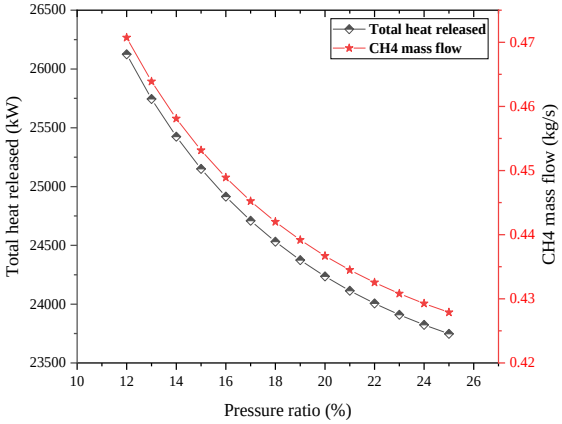

Fig. 9. GT PR to gas burner total heat released and CH_4 mass flow.

The results show that with a higher GT pressure ratio, the CH_4 mass flow required to satisfy the optimization process declines and hence less total heat releases in the combustion process. The decrease in these parameters explains the decline in the thermal capacity of the ORC-EVAP, as shown in Fig. 8.

Fig. 10 shows the effect of increasing the GT pressure ratio on the final water temperature and GT working fluid (air) temperature at State 3. Although the overflow in power, due to the GT pressure ratio increment, is used to maintain the constant net power output of (5335 kW) instead of increasing the final water temperature, the results show that the temperature of water and air declines slightly. In addition, the modeling procedure has maintained a PPT of 3 ºC between the two working fluids at the end of HX1.

The results support that the final water temperature value of between 60-67 ºC is still appropriate for heating applications.

Theoretically speaking, increasing GT- pressure ratio should increase GT-efficiency [36]. To verify this, the effect of increasing the GT pressure ratio on the GT efficiency is presented in Fig. 11.

This study supports that increasing the GT pressure ratio results in a higher GT cycle efficiency. For the selected pressure ratio range, the cycle efficiency increases from 20% to 22.5%. As the net power output of the GT cycle is maintained constant throughout the modeling procedure, increasing the GT-pressure ratio results in a decline in CH_4 mass flow and its total thermal energy releases in the combustion chamber (see Fig. 9). Therefore, the GT efficiency increases.

6. Model validation

As far as the author knowledge, there is no similar experimental or theoretical study in the open literature on a similar cycle configuration for co-generation of power and hot water supply. Thus, the validation of this work is based on individual sub-cycle of this combined system. For the GT cycle, the working conditions are adopted from a real cycle, as provided in Table 1 [28].

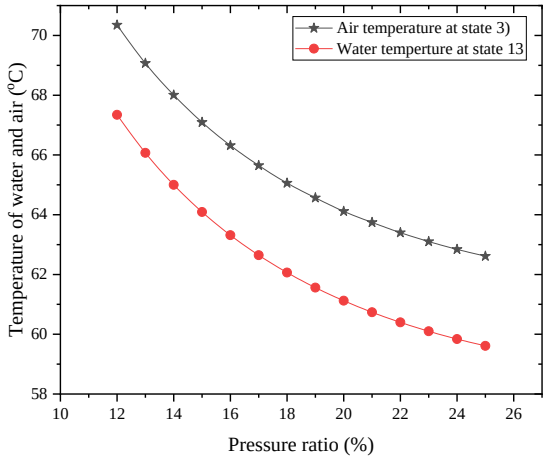

Fig. 10. GT PR to air and water temperature.

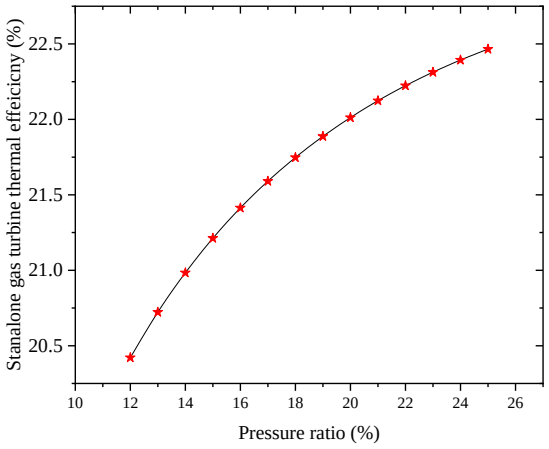

Fig. 11. Standalone gas turbine PR to efficiency.

The exhaust temperature adopted in this study is 900 ºC to maximize the GT output efficiency, as indicated in Table 2. In this study, a similar net power output of 5335 kW is achieved by adjusting other designed parameters, such as working fluid mass flow rate (Table 3). For the ORC validation, the results of this study are compared with experimental and simulation study conducted by Collings *et al.* [37] using R245fa as working fluid, with a condenser pressure of 1.6 bar for a system used for power generation. The reference study has achieved cycle efficiency of 6.8% experimentally compared to 8.2% theoretically under the same PR of 4.1. In the current study, higher PR of 7.2 is adopted with a condenser pressure of 5 bar, aiming to achieve higher theoretical ORC efficiency of 11.5% for power and heating output. The percentage deviation in the pressure

ratio between these two studies is around 43%, which corresponds to the percent deviation of the ORC efficiency of 41% achieved experimentally. Furthermore, the overall thermal efficiency of the combined cycle is 51.5%, which is in good agreement with the overall thermal efficiency of the combined system adopted by 54.4% Mahdavi *et al.* [38]. Finally, the proposed system can heat water from 10 ºC to 65 ºC for domestic heating application, which is similar to the results achieved by Liang *et al.* [32].

7. Conclusions

The thermodynamic analysis is carried out on a combined heat and power system that integrates GT, ORC, and a heat exchanger. The concept is based on recovering the wasted heat from the gas turbine to produce additional heat load and mechanical power to enhance the overall efficiency of the integrated system. Two combined cycle configurations are investigated and compared in this study, the only difference is the heated water route through the system. The steady-state results show the following outcomes:

- The combined system converts 51.55% of the total heat released from fuel combustion in the GB into useful energy modes compared to the standalone GT cycle, which achieved only 21%.
- The mechanical efficiency of the combined system increases to 24% by adding the recovered ORC net power to the overall power production. The rest of the recovered energy (27.55%) is utilized to generate hot water at a temperature of 65 ºC.
- There is still a significant amount of thermal energy (48.45%) lost mainly through the combustion process with a small ratio lost through the exhaust line (3.5%). For future studies, the lost thermal energy through the combustion process has the potential to be recovered into a useful energy mode.
- The comparison between models (A) and (B) shows no difference in the overall combined thermal efficiency and the final hot water temperature.

The results of varying gas turbine PR are:

- Increasing the GT pressure ratio increases both GT turbine and compressor work. The compressed air temperature after State 2 also increases, which enhances the HX1 thermal capacity. The advantage of adding a heat exchanger between the GT compressor and gas burner is to recover the heat from the high thermal energy fluid in Stream 2. The resultant low-temperature compressed air outlet can carry more heat from the combustion process, contributing to less heat lost in the combustion chamber.
- The system mass flow rate reduces, requiring smaller equipment sizing, leading to saving initial costs.
- The total net power output increases by 11.5-16% over the designed GT net power output.
- The thermal energy rejected by the environment reduces by 9.5%.
- Although a higher pressure ratio results in increasing GT efficiency from 20% to 22.5%, the final water temperature reduces from 67 ºC to 60 ºC, which is still suitable for various heating needs.

References

[1] F. Birol, "Key World Energy Statistics", *IEA*, pp. 6-7, (2021).

[2] S. Nalley, "Annual Energy Outlook 2022 with projections to 2050". *US Energy Information Administration*, (2022).

[3] M. Al-Tameemi, *Thermal analysis of combined Organic Rankine-Vapour compression system for heating and cooling applications*, PhD thesise, University of Glasgow, (2019).

[4] H. Jouhara, N. Khordehgah, S. Almahmoud, B. Delpech, A. Chauhan and S. Tassou, "Waste heat recovery technologies and applications", *Therm. Sci. Eng. Prog.*, Vol. 6, pp. 268–289, (2018).

[5] J. Nondy and T.K. Gogoi, "Tri-objective optimization of two recuperative gas turbine-based CCHP systems and 4E analyses at optimal conditions", *Appl. Energy*, Vol. 323, p. 119582, (2022).

[6] S. Sanaye, M. Meybodi and S. Shokrollahi, "Selecting the prime movers and nominal powers in combined heat and power systems", *Appl. Therm. Eng.*, Vol. 28, No. 10, pp. 1177–1188, (2008).
[7] M. Valenti, "Reaching for 60 percent", *Mechanical Engineering*, Vol. 124, No. 4, pp. 35-39, (2002).
[8] D. Robb, "CCGT: Breaking the 60 per cent efficiency barrier", *Power Engineering International*, Vol. 18, No. 3, pp. 28-32, (2010).
[9] M. Eke, P. Ozor, V. Aigbodion, C. Mbohwa, "Second law approach in the reduction of gas emission from gas turbine plant", *Fuel Commun*, Vol. 9, p. 100030, (2021).
[10] A. Valero, M. Lozano, L. Serra, G. Tsatsaronis, J. Pisa, C. Frangopulos and M. Spakovsky, "CGAM Problem: definition and conventional solution", *Energy*, Vol. 19, No. 3, pp. 279–286, (1994).
[11] A., Aghaei, and R. Saray, "Optimization of a combined cooling, heating, and power (CCHP) system with a gas turbine prime mover: A case study in the dairy industry", *Energy*, Vol. 229, p. 120788, (2021).
[12] S. Kang, H. Li, J. Lei, L. Liu, B. Cai and . Zhang, "A new utilization approach of the waste heat with mid-low temperature in the combined heating and power system integrating heat pump", *Appl. Energy*, Vol. 160, pp. 185-193, (2015).
[13] B. Cai, H. Li, Y. Hu, L. Liu, J. Huang, A. Lazzaretto and G. Zhang, "Theoretical and experimental study of combined heat and power (CHP) system integrated with ground source heat pump (GSHP)", *Appl. Therm. Eng.*, Vol. 127, pp. 16-27, (2017).
[1] D. Balanescu and V . Homutescu, "Perfromnace analysis of a gas turbine combined cycle power plant with waste heat recovery in Organic Rankine Cycle", *The 12th Int. Conference Interdisciplinarity in Engineering*, Tirgu Mures, Romania, Vol. 32, pp. 520–528, (2019).
[15] C. Diyoke, U. Ngwaka and T. Onah, "Comparative assessment of a hybrid of gas turbine and biomass power system for sustainable multi-generation in Nigeria", *Sci. Afr.*, Vol. 13, p. e00899, (2021).
[16] Z. Wang, W. Han, N. Zhang, M. Liu and H. Jin, "Proposal and assessment of a new CCHP system integrating gas turbine and heat-driven cooling/power cogeneration", *Energy Convers. Manage.*, Vol. 144, pp. 1–9, (2017).
[17] X. Zhao, L. Fu, X. wang, T. Sun, J. Wang and S. Zhang, "Flue gas recovery system for natural gas combined heat and power plant with distributed peak-shaving heat pumps", *Appl. Therm. Eng.*, Vol. 111, pp. 599-607, (2017).
[18] H. Lei, H. Dongjiang, Y. Jinfu, T. Changliang and L. Hao, "Study on different heat supplementation strategies for a combined cooling, heating and power system", *Appl. Therm. Eng.*, Vol. 144, pp. 558-570, (2018).
[19] M. Farahbakhsh, and M. Chahartaghi, "Performance analysis and economic assessment of a combined cooling heating and power (CCHP) system in wastewater treatment plants (WWTPs)", *Energy Convers. Manage.*, Vol. 224, p. 113351, (2020).
[20] Z. Huang, K. Soh, M. Islam and K. Chua, "Digital twin driven life-cycle operation optimization for combined cooling heating and power-cold energy recovery (CCHP-CER) system", *Appl. Energy*, Vol. 324, p. 119774, (2022).
[21] J. Wang, Z. Lu, M. Li, N. Lior and W. Li, "Energy, exergy, exergoeconomic and environmental (4E) analysis of a distributed generation solar-assisted CCHP (combined cooling, heating and power) gas turbine system", *Energy*, Vol. 175, pp. 1246-1258, (2019).
[22] N. Mahdavi, P. Mojaver and S. khalilarya, "Multi-objective optimization of power, CO2 emission and exergy efficiency of a novel solar-assisted CCHP system using RSM and TOPSIS coupled method", *Renewable Energy*, Vol. 185, pp. 506-524, (2022).
[23] Moafi Madani, S. M., Alinejad, J., Rostamiyan, Y., & Fallah, K., "Numerical

study of geometric parameters effects on the suspended solid particles in the oil transmission pipelines", *Proceedings of the Institution of Mechanical Engineers. Part C, Journal of Mechanical Engineering Science*, Vol. 236, No. 8, pp. 3960-3973, (2022)

[24] J. Alinejad, N. Montazerin, S. Samarbakhsh, "Accretion of the efficiency of a forward-curved centrifugal fan by modification of the rotor geometry: Computational and experimental study", *International Journal of Fluid Mechanics Research*, Vol. 40, No. 6, pp. 469-481, (2013).

[25] M. Peiravi, J. Alinejad, "3D numerical simulation of fibers arrangement effects on thermal conductivity of polymer matrix composite", *Mechanics of Advanced Compsite Structures*. Vol. 9, No. 1, pp. 59-73, (2022).

[26] J. Alinejad and E. J. A. Esfahani, "Numerical stabilization of three-dimensional turbulent natural convection around isothermal cylinder", *J. Thermophys. Heat Trans.*, Vol. 30, No. 1, pp. 94-102, (2016).

[27] J. Alinejad and E. J. A. Esfahani, "Lattice-Boltzmann simulation of forced convection over an electronic board with multiple obstacles", *Heat Transfer Research.* Vol. 45, No. 3, pp. 241-262, (2014).

[28] R. Farmer, B. deBiasi, J. Isles, H. Jaeger, M. Asquino, M. Cornett, J. Hanson and V. deBiasi, "Gas Turbine World 2014 Performance Specs, 30th edition", Vol. 44, No. 1, (2014).

[29] Aspen plus v10 , Aspen Technology Inc.:USA.

[30] Lemmon, E. et al, "NIST Reference Fluid Thermodynamic and Transport Properties Database (REFPROP), Version 9.1.

[31] M. Al-Tameemi, Y. Liang and Z. Yu, "Design Strategies and Control Methods for a Thermally Driven Heat Pump System Based on Combined Cycles", *Front. Energy Res.*,Vol. 7, p. 131, (2019).

[32] Y. Liang, M. Al-Tameemi and Z. Yu, "Investigation of a gas-fuelled water heater based on combined power and heat pump cycles", *Appl. Energy*, Vol. 212, pp. 1476-1488, (2018).

[33] M. Al-Tameemi, Y. Liang and Z. Yu, "Combined ORC-HP thermodynamic cycles for DC cooling and waste heat recovery for central heating", *Energy Procedia*, Vol. 158, pp. 2046-2051, (2019).

[34] P. Collings, M. Al-Tameemi and Z. Yu, "A Combined Organic Rankine Cycle-Heat Pump System for Domestic Hot Water Applications", "*12th Int. Conference on Heat Transfer, Fluid Mechanics and Thermodynamics*", Malaga, Spain, (2016).

[35] A. Emamifar, "Thermodynamic analysis of a hybrid absorption two-stage compression refrigeration system employing a flash tank with indirect subcooler", *Journal of Computational and Applied Research in Mechanical Engineering*. Vol. 12, No. 2, pp. 145-159 (2013).

[36] Y. Çengel, M. Boles and M. Kanoğlu, *Thermodynamics An engineering approach, Ninth edition*, McGraw-Hill Education, New York, NY, pp. 497-500 (2019).

[37] Collings, P.; Mckeown, A.; Wang, E.; Yu, Z, "Experimental Investigation of a Small-Scale ORC Power Plant Using a Positive Displacement Expander with and without a Regenerator", *Energies*, Vol. 12, No. 8, 1452, (2019).

[38] N. Mahdavi, P. Mojaver and S. Khalilarya, "Multi-objective optimization of power, CO2 emission and exergy efficiency of a novel solar-assisted CCHP system using RSM and TOPSIS coupled method", *Renewable Energy*, Vol. 185, pp. 506-524, (2022).

Copyrights ©2023 The author(s). This is an open access article distributed under the terms of the Creative Commons Attribution (CC BY 4.0), which permits unrestricted use, distribution, and reproduction in any medium, as long as the original authors and source are cited. No permission is required from the authors or the publishers.

How to cite this paper:

Mohammed Ridha Jawad Al-Tameemi, Samir Gh. Yahya, Saadoon Abdul Hafedh and Itimad D. J. Azzawi, "Thermodynamic optimization of an integrated gas turbine cycle, heat exchanger and organic Rankine cycle for co-generation of mechanical power and heating load,", *J. Comput. Appl. Res. Mech. Eng.*, Vol. 13, No. 1, pp. 75-88, (2023).

DOI: 10.22061/JCARME.2023.9366.2253

URL: https://jcarme.sru.ac.ir/?_action=showPDF&article=1872